



Published in final edited form as:

Nat Cancer. 2021 August ; 2(8): 794–802. doi:10.1038/s43018-021-00232-6.

Mature tertiary lymphoid structures predict immune checkpoint inhibitor efficacy in solid tumors independently of PD-L1 expression

Lucile Vanhersecke, MD^{1,2,¥}, Maxime Brunet, MD^{2,3,¥}, Jean-Philippe Guégan, PhD⁴, Christophe Rey, PhD⁴, Antoine Bougouin, MSc⁵, Sophie Cousin, MD³, Sylvestre Le Moulec, MD⁶, Benjamin Besse, MD⁷, Yohann Lorient, MD⁷, Mathieu Larroquette, MD^{2,3}, Isabelle Soubeyran, MD, PhD¹, Maud Toulmonde, MD, PhD³, Guilhem Roubaud, MD³, Simon Pernot, MD, PhD³, Mathilde Cabart, MD³, François Chomy, MD³, Corentin Lefevre, MD³, Kevin Bourcier, MD³, Michèle Kind, MD⁸, Ilenia Giglioli, MSc⁵, Catherine Sautès-Fridman, PhD⁵, Valérie Velasco, MSc¹, Félicie Courgeon, PharmD, MSc⁴, Ezoglin Oflazoglu, MD, PhD⁹, Ariel Savina, PhD⁹, Aurélien Marabelle, MD PhD⁷, Jean-Charles Soria, MD⁷, Carine Bellera, PhD¹⁰, Casimir Sofeu, PhD¹⁰, Alban Bessede, PhD^{4,¥}, Wolf H. Fridman, MD, PhD^{5,¥}, François Le Loarer, MD, PhD^{1,2,¥}, Antoine Italiano, MD, PhD^{2,3,7,¥}

¹Department of Pathology, Institut Bergonié, Bordeaux, France

²Faculty of Medicine, University of Bordeaux, Bordeaux, France

³Department of Medicine, Institut Bergonié, Bordeaux, France

⁴Explicyte Immuno-Oncology, Bordeaux, France.

Corresponding author: Pr. Antoine ITALIANO, Early Phase Trials and Sarcoma Units, Institut Bergonié, a.italiano@bordeaux.unicancer.fr, Pr. Antoine ITALIANO, Gustave Roussy, antoine.italiano@gustaveroussy.fr.

[¥]L.V; M.B; A.B., W.H.F., F.L.L., and A.I. contributed equally to this work

AUTHOR CONTRIBUTIONS

AI, AB, WHF, and FLL conceived and designed the study. LV and FLL performed the histological analyses. SC, SLM, IS, MT, GR, SP, MC, FC, CL, KB, MK, FC, BB, YL, AM, JCS, and AI provided study material or treated patients. All authors collected and assembled data. AI, AB, LV, and FLL developed the tables and figures. AI, AB, MB, FLL, WHF, and CSF conducted the literature search and wrote the manuscript. All authors were involved in the critical review of the manuscript and approved the final version.

DECLARATION OF INTERESTS

LV, MB, SC, SLM, ML, IS, MT, GR, SP, MC, FC, CL, KB, MK, IG, CSF, VV, FC, WHF, and FLL: Nothing to disclose

AB, JPG, and CR: Employees of Immusmol/Explicyte

EO, AS: Employees of Astra Zeneca

AI: Received research grants from Astra Zeneca, Bayer, BMS, Chugai, Merck, MSD, Pharmamar, Novartis, Roche, and received personal fees from Epizyme, Bayer, Lilly, Roche, and Springworks

BB: Received grants from AstraZeneca, Pfizer, Eli Lilly, Onxeo, Bristol Myers Squibb, Inivata, Abbvie, Amgen, Blueprint Medicines, Celgene, GlaxoSmithKline, Ignyta, Ipsen, Merck KGaA, MSD Oncology, Nektar, PharmaMar, Sanofi, Spectrum Pharmaceuticals, Takeda, Tiziana Therapeutics, Cristal Therapeutics, Daiichi Sankyo, Janssen Oncology, OSE Immunotherapeutics, BeiGene, Boehringer Ingelheim, Genentech, SERVIER, Tolero Pharmaceuticals

YL: Received grants and personal fees from Janssen, during the conduct of the study; personal fees and non-financial support from Astellas, grants and personal fees from Sanofi, personal fees and non-financial support from Roche, personal fees and non-financial support from AstraZeneca, grants, personal fees and non-financial support from MSD, personal fees and non-financial support from BMS, personal fees from Clovis, personal fees and non-financial support from Seattle Genetics, personal fees from Incyte, personal fees from Pfizer.

AM: Received research grants from Mersu, Bristol-Myers Squibb, Boehringer Ingelheim, Transgene, MSD and received personal fees from Bristol-Myers Squibb, AstraZeneca, MedImmune, Oncovir, Merieux

JCS: Has received consultancy fees from AstraZeneca, Astex, Clovis, GSK, GamaMabs, Lilly, MSD, Mission Therapeutics, Merus, Pfizer, Pharma Mar, Pierre Fabre, Roche/Genentech, Sanofi, Servier, Symphogen, and Takeda.

⁵Centre de Recherche des Cordeliers, INSERM, Sorbonne Université, USPC, Université de Paris, Paris, 75006 France.

⁶Clinique Marzet, Department of Oncology, Pau, France

⁷Gustave Roussy, Department of Medicine, Villejuif, France

⁸Department of Radiology, Institut Bergonié, Bordeaux, France

⁹Astra Zeneca, Rahway, New Jersey, USA

¹⁰Clinical Research and Clinical Epidemiology Unit (ISO 9001 Certified), Institut Bergonié, Comprehensive Cancer Centre, 229 Cours de l'Argonne, 33076 Bordeaux, France

Abstract

Only a minority of patients derive long-term clinical benefit from anti-PD1/PD-L1 monoclonal antibodies. The presence of tertiary lymphoid structures (TLS) has been associated with improved survival in several tumor types. Here, using a large-scale retrospective analysis of three independent cohorts of cancer patients treated with anti-PD1/PD-L1 antibodies, we showed that the presence of mature TLS was associated with improved objective response rate, progression-free survival, and overall survival independently of PD-L1 expression status and CD8+ T-cell density. These results pave the way for using TLS detection to select patients who are more likely to benefit from immune checkpoint blockade.

Keywords

Immune checkpoint inhibitors; biomarkers; tertiary lymphoid structures (TLS); tumor microenvironment

The discovery of immune inhibitory checkpoints has revolutionized the systemic approach to cancer treatment. The programmed death 1 (PD-1) inhibitory checkpoint has played a key role in understanding how tumors can evade immune surveillance. Blocking the interaction between the PD-1 receptor and its primary ligand (PD-L1) has demonstrated remarkable anticancer activity and has led to the recent approval of anti-PD-1/PD-L1 drugs for several solid tumor types¹. However, most patients receiving anti-PD-1/PD-L1 monoclonal antibodies do not derive benefit. Hence, there is a crucial need to identify reliable predictive biomarkers of the response to anti-PD-1/PD-L1 agents to develop precision medicine for cancer immunotherapy.

PD-L1 expression status as assessed by immunohistochemistry, tumor mutational burden, and microsatellite instability status are so far the sole companion diagnostic markers approved to guide anti-PD1 therapy². However, all of them, particularly PD-L1 expression, are imperfect predictors of a patient's response to immune checkpoint inhibition, as demonstrated by discordant results reported by multiple studies and the varied and evolving scoring systems that have been devised for different tumor types². In addition to CD8+ T cells, other immune cell populations may impact the efficacy of anti-PD1/PD-L1 antibodies. Several studies have indeed shown that tumor-associated macrophages and tumor-associated neutrophils are associated with resistance to anti-PD1 therapy in multiple tumor types^{3,4}. B

cells localized in so-called tertiary lymphoid structures (TLS) may also play a crucial role in the tumor immune microenvironment. TLS can be likened to micro-secondary lymphoid organs. Mature TLS are composed of prominent B-cell follicles and follicular dendritic cells that are adjoined to a smaller T-cell zone containing a mixture of CD4+ and CD8+ T cells⁵. TLS have been identified in several solid tumor types and are associated with better survival when present in the tumor microenvironment⁵⁻⁸. Higher densities of TLS were associated with an increased density of tumor-infiltrating CD8+ T lymphocytes⁹⁻¹⁰ and with an activated and cytotoxic immune signature⁸. We and others have recently reported that the expression of B cells and TLS gene signatures were predictive of improved outcomes in sarcoma and melanoma patients treated with immune checkpoint inhibitors^{11,12,13}. Altogether, these data suggest that TLS may be crucial for an effective antitumor immune response. We therefore decided to investigate the predictive value of TLS in patients treated with anti-PD1/PD-L1 antagonist and validated its assessment in a routine diagnostic setting.

RESULTS

We analyzed tumor samples obtained before immunotherapy onset from 328 patients (Discovery cohort) treated with anti-PD1 or anti-PD-L1 monoclonal antibodies who were included prospectively in an institutional tumor profiling program (NCT02534649). The patient characteristics are summarized in Supplementary Table 1. For each case, the TLS status was assessed by two pathologists blinded to the clinical data. We observed the presence of TLS in 105 cases (32%), including 84 cases with mature TLS (25.6%) (mTLS, as defined by the presence of CD23+ follicular dendritic cells within the TLS structure) (Fig. 1a, Extended Data Fig. 1b). Baseline characteristics were not significantly different between patients according to their TLS status (Table 1). TLS were present across all the tumor histotypes (Table 1).

Thirty-one of 84 patients (36.9%; 95% CI, 26.6%–48.1%) in the mature TLS group had an objective response compared with 4 out of 21 patients (19.3%; 95% CI, 5.4%–41.9%) with immature TLS and 43 out of 223 patients (19%; 95% CI, 14.3%–25.1%) in the TLS-negative group, $p=0.015$ (Fig. 1b).

Regardless of the efficacy endpoint analyzed, the proportion of patients with mature TLS-positive tumors was significantly higher among those displaying clinical benefit. The proportion of patients with mature TLS-positive tumors was significantly higher in patients with an objective response according to Response Evaluation Criteria in Solid Tumors (RECIST) (39.7%) than in patients with stable disease (16.9%) or progressive disease (23.4%), $p=0.015$. Sixty patients (18.3%) were long-term survivors (overall survival 24 months). The proportion of patients with mature TLS among long-term survivors was significantly higher than in the other patient group: 40% versus 22.4%, $p=0.005$ (Fig. 1c).

The median follow-up was 25.1 months. The median PFS was 6.1 (95% CI, 2–10.2) months in the mature TLS positive group and 2.7 (95% CI, 1.9–3.5) months in the TLS-negative group, $p=0.015$ (Fig. 1d). The 6-month, 1-year, and 2-year PFS rates were 51.7%, 37.9%, and 27.0% in the mature TLS positive group and 34.4%, 22.1%, and 11.3% in the negative mature TLS group, respectively.

At the time of analysis, 211 patients (64.3%) had died and 117 (35.7%) were still alive. The median overall survival (OS) was 24.8 (95% CI, 6.8–42.8) months in the mature TLS positive group and 13.3 (95% CI, 11.1–15.5) months in the TLS-negative group, $p=0.016$ (Fig. 1d). The 6-month, 1-year, and 2-year OS rates were 82.6%, 66.3%, and 52.7% in the mature TLS positive group and 76.6%, 53.7%, and 30.3% in the TLS-negative group.

We then analyzed within the discovery cohort the correlation between PD-L1 expression scores, CD8+ T-cell infiltration, TLS status, and patient outcomes. The PD-L1 tumor proportion score (TPS) was $\geq 1\%$ in 70 patients (21.3%). The proportion of PD-L1-positive tumors was similar among tumors with a high density of mature TLS (22.4%) and those with a low density or absent mature TLS (21.1%). Regardless of the PD-L1 expression status, patients with mature TLS positive tumors had a better outcome. Among patients with PD-L1-positive tumors (i.e., PD-L1 TPS $\geq 1\%$) and PD-L1-negative tumors (i.e., PD-L1 TPS $< 1\%$), the objective response rates in patients with a mature TLS positive tumors were, respectively, 69.2% (95% CI, 38.6%–91%) and 40.3% (95% CI, 27.6%–54.2%) versus 35.6% (95% CI, 21.9%–51.2%) and 14.1% (95% CI, 9.7%–19.4%) for patients with mature TLS negative tumors, $p=0.001$ (Fig. 2b and 2c, Table 2). Similar results were obtained for the PD-L1 combined positive score (CPS) (Table 2). Among patients with a PD-L1 TPS $< 1\%$, the median PFS and OS were, respectively, 4.8 (95% CI, 2.4–7.2) and 18.6 (95% CI, 4.6–32.5) months in the mature TLS positive group versus 2.6 (95% CI, 1.9–3.3) and 12.7 (95% CI, 10–15.3) months in the mature TLS-negative group; overall log-rank test $p=0.013$ (PFS) and $p=0.018$ (OS). Among patients with a PD-L1 TPS $\geq 1\%$, the median PFS and OS were, respectively, 31 (95% CI, 6.5–55.4) and 62 (95% CI, 0–131) months in the mature TLS positive group versus 5.6 (95% CI, 1.8–9.4) and 16.4 (95% CI, 12.6–20.1) months in the /mature TLS-negative group, overall log-rank test $p=0.013$ (PFS) and $p=0.018$ (OS) (Fig. 2b and 2c). Similar results were obtained for the PD-L1 CPS score (Extended Fig. 2).

The median density of CD8+ T cells was 123/mm². The proportion of high CD8+ T-cell density cases (above the median) significantly correlated with the TLS status: 45% in TLS-negative cases versus 72% in the TLS-positive group, $p=0.0001$. Presence of mature TLS was significantly associated with an improved objective response rate (Table 2), PFS, and OS in the high CD8+ T-cell density group, whereas no significant difference was observed in the low CD8+ T-cell density group (Extended Fig. 3).

As shown in Supplementary Table 2 and Table 3, the multivariate analysis showed that the presence of mature TLS was the most significant predictive factor for objective response and had an independent predictive value for both PFS and OS when adjusted with other prognostic factors including the performance status, the PD-L1 TPS score, and the level of CD8+ T-cell infiltration (Table 3).

To confirm that our results were representative of all cancer types studied, we performed one additional analysis by removing non-small-cell lung cancer (NSCLC) patients (the most frequent histology). We observed a significantly higher objective response rate in mature TLS-positive tumors than in other tumors (41.2% versus 11.4%, $p<0.0001$), as well as improved PFS (4.8 versus 2.3 months, $p=0.018$) and OS (18.6 versus 12.5 months, $p=0.048$).

These results indicate that the predictive value of TLS was not solely driven by the NSCLC histology (Extended Fig. 4).

To confirm the robustness of the predictive value of TLS across different health care settings, we analyzed two additional independent validation cohorts. The first one (Validation cohort A) included 131 cancer patients who were treated in a community setting. We observed the presence of mature TLS in 44 cases (33.6%), and the median follow-up was 14.9 months. We found a significantly higher objective response rate (50% vs 27.6%, $p=0.009$) and PFS (8 vs 3.5 months, $p=0.038$) and a trend of improvement in overall survival in the mature TLS-positive group (37.3 vs 26.9 months, $p=0.105$) (Fig. 2d). The second validation cohort (Validation cohort B) included 81 patients from the MATCH-R study ([NCT02517892](#)), which was a prospective study specifically designed to investigate biomarkers of sensitivity and resistance to anticancer agents. In this study, all the patients underwent a single biopsy from one metastatic site immediately before immunotherapy onset. We observed the presence of mature TLS in 13 cases (16%). Again, we found that patients with mature TLS-positive tumors had a significantly better outcome than patients with no mature TLS, with an objective response rate of 38.4% vs 11.8%, $p=0.02$; a median PFS of 10.9 vs 2.1 months, $p=0.079$; and a median OS of 24.6 vs 8.1 months, $p=0.036$ (Fig. 2e).

Because patients from Validation cohort B consented to genetic analysis, we decided to explore the correlation between TLS status and the tumor mutational burden (TMB). Among the 81 patients in Validation cohort B, 70 (86.4%) had evaluable TMB scores, 10 had TMB-high status (14.3%), and the remaining 70 patients (85.7%) had non-TMB-high status. The objective response rate in the TMB-high group was 30% versus 15% in the TMB-low group, although this difference did not reach statistical significance. No significant difference in terms of PFS (6.8 vs 2.1 months, $p=0.34$) or OS (16.2 vs 10.2 months, $p=0.75$) was observed between the two groups. The proportion of patients with mature TLS was not significantly different between the two groups (10% versus 16.5%, $p=0.6$).

Our results indicate that the presence of mature TLS predicts an improved objective response and improved PFS and OS in cancer patients treated with immune checkpoint inhibitors independently of PD-L1 status and CD8+ T-cell infiltration level.

We and others have recently provided indirect evidence that B-cell infiltration through TLS is associated with better outcomes in cancer patients treated with immunotherapy. By analyzing the gene expression profile of 47 samples from soft-tissue sarcoma patients treated with the PD1 antagonist, we demonstrated an improved response rate in tumors with a high expression of B-cell lineage genes (50% versus 13.5%, $p=0.01$)¹¹. Cabrita et al. also showed that a gene signature associated with TLS was predictive of clinical outcomes in three independent cohorts of melanoma patients treated with anti-CTLA4 ($n=37$, $n=40$) or anti-PD1 monoclonal antibodies ($n=40$)¹². In both studies, additional samples were analyzed to confirm that the B gene expression signature correlated with the presence of TLS in tumors.

Helmink et al. analyzed the predictive value of TLS in two cohorts—23 melanoma patients and 19 renal cell carcinoma patients¹³. The density of TLS to tumor was higher in

responders than in non-responders in both cohorts, although statistical significance was not reached given the limited sample size of the study¹³.

In this pan-tumor study, we were able to identify TLS across 11 different tumor types and demonstrate that their presence correlates with immunotherapy efficacy.

Moreover, we show that pathological analysis can reliably detect TLS in tumor samples. Although the maturity of TLS was assessed by immunofluorescence in this study to enable a multiparametric analysis, we also implemented dual CD20-CD23 immunostaining, which is readily accessible in routine pathology laboratories. This assessment yielded the same results as those obtained by immunofluorescence in 91.9% of cases (n=57/62, Supplementary Table 3).

Altogether, our results strongly support a role for B cells within TLS in the response to PD1/PD-L1 antagonists in cancer patients. To add further complexity, the role of B cells in the tumor microenvironment through the secretion of antibodies and cytokines, the modulation of T-cell function, and the regulation of antigen processing and presentation¹⁴ may be pro- or anti-tumorigenic depending on whether they are involved in immature or mature TLS¹⁵. In immature TLS, B cells may produce molecules released in the tumor microenvironment or expressed on their membrane that impair an efficient antitumor immune response. By contrast, in mature TLS, B cells may instruct CD8+ T cells by presenting them tumor-derived antigen¹⁶. Although the precise mechanism by which mature TLS control tumor growth and predict the response to checkpoint blockade is not fully understood, it is established that plasma cells are generated in TLS germinal centers¹⁶⁻¹⁷.

Plasma cells may produce antitumor antibodies¹⁷⁻¹⁸ that form antigen-antibody complexes with tumor-associated antigens, the latter being internalized by dendritic cells resulting in very efficient antigen presentation to T cells¹⁹. This amplification mechanism should allow a much more efficient activation of CD8+ T cells in the tumor microenvironment, particularly in the context of immune checkpoint blockade²⁰. Notably, we found that the response rate of immature TLS tumors was not different from that of TLS-negative tumors and that mature TLS-positive tumors were more infiltrated by CD8+ T cells. Pre-existing T-cell antitumor immunity has been hypothesized as a prerequisite to the anti-PD1/PD-L1 response. Interestingly, we found that the presence of mature TLS was significantly associated with improved outcomes in tumors with a high infiltration of CD8+ T cells, whereas outcomes were poor for patients with tumors poorly infiltrated by CD8+ T cells regardless of the TLS status. This suggests that the presence CD8+ T cells is necessary but not sufficient to induce a sustained antitumor immune response, which indeed requires crucial cooperation with B cells. These T cells may become exhausted, explaining why treatment with anti-PD1/PD-L1 antagonist may result in substantial efficacy in tumors enriched in mature TLS.

One main limitation of our study was its retrospective design. However, thanks to a robust methodology (multicentric setting, large sample size, blinded assessment of the microenvironment profile and the TLS maturity characterization), our findings indicate that when present before treatment, TLS could be considered as a predictor of patient response

to immunotherapy. Moreover, mature TLS status was associated with improved outcomes irrespective of PD-L1 expression, with mature TLS status enriching for improved response and survival in both PD-L1-positive and PD-L1-negative patients, particularly in the latter group, which is the most important in terms of prevalence. Additionally, the predictive value of mature TLS did not appear to be driven by a particular tumor type, with an increased proportion of patients with better outcomes being observed across most tumor types.

Whether the formation of TLS can be induced by specific therapies to improve patient outcomes is also an important question to address. Lu et al. have recently demonstrated that TLS emerge after neoadjuvant chemotherapy in breast cancer and that these TLS contain a specific subset of B cells playing a key role in antitumor T-cell immunity induction and response to chemotherapy²¹. Interestingly, Helmink et al. also observed that treatment with immune checkpoint inhibitors can favor the emergence of TLS and showed that patients with more abundant TLS in post-treatment tumor samples were more likely to respond to treatment¹³.

For patients with advanced tumors, there is an unmet medical need for treatment options. Our results provide direct evidence of the crucial role of mature TLS in response to immunotherapy. These findings pave the way for using TLS as a biomarker to select patients who are more likely to benefit from immune checkpoint inhibition. Ongoing clinical trials are evaluating this innovative approach in sarcoma patients ([NCT02406781](#); [NCT04095208](#)).

METHODS

Patients

This study was based on retrospectively retrieved data from the medical records of three independent cohorts of patients treated between December 2013 and May 2019 in an academic setting (Discovery: Institut Bergonié, Bordeaux, France, [NCT02534649](#), Validation cohort B: Gustave Roussy, Villejuif, France) and in a community setting (Validation cohort A: Clinique Marzet, Pau, France). The inclusion criteria were age 18 years, histologically proven malignant tumor, unresectable and/or metastatic disease, at least one tumor evaluation by imaging after immunotherapy onset, and availability of paraffin-embedded tumor material obtained before immunotherapy onset. Institutional ethics review board approval and patient informed consent were obtained for this study.

Treatments and evaluation

Patients were treated at the discretion of their physician. The best response to treatment was evaluated according to Response Evaluation Criteria in Solid Tumors (RECIST) after central review²². Routine follow-up was similar across the two centers involved in the study. PFS was defined as the time from the start of treatment until disease progression, death, or last patient contact. OS was defined as the time from the start of treatment until death or last patient contact.

TLS screening in pathology (Figure 1)

All cases were reviewed blindly by 2 pathologists (LV, FLL) for the presence and state of maturity of TLS according to the hematoxylin eosin saffron (HES), the immunohistochemical and immunofluorescence stainings on serial sections. The samples analyzed were biopsies (discovery cohort: n=213, 65%; validation cohort A: n=85, 64.9%; discovery cohort B: n=81, 100%) or surgical samples (discovery cohort: n=115, 35%; validation cohort A: n=46, 33.1%; discovery cohort B: n=0, 0%). The pathological screening was validated with an independent set of 138 tumor samples that were scored blindly by both the pathologists (FLL, LV) and the immunologists (AB, IG, CSF, WHF) (Extended Figure 5, Supplementary Table 3). For the rare discordant cases (n=9/138), the final TLS status of samples was agreed upon consensually with a board gathering both teams (Supplementary Table 3). The diagnostic criteria used to determine the TLS status were inferred from this training set and were validated by both pathology and immunology teams, derived and adapted from the initial method by Petitprez et al.¹¹ TLS were defined as lymphoid aggregates of B lymphocytes (admixed with a variable proportion of plasma cells and T lymphocytes in most cases). Only TLS made up of more than 50 cells were included in the analysis. TLS were considered significant when located either among the tumor cells or at the invasive margin (defined as fibrous tissue distant of less than 1mm from tumor cells), as previously described⁹. When the TLS status was assessed on lymphoid organs (namely lymph nodes, spleen, tonsils), TLS were only taken into account when admixed to tumor cells and if distant from the residual parenchyma, to exclude pre-existing lymphoid follicles. TLS were classified as “mature” when at least one CD23+ dendritic cell was detected in the TLS. When isolated CD23-positive cell were detected, the cells had to display a dendritic morphology (i.e. cytoplasmic “dendritic” extensions) to be considered significant. In the absence of CD23 positivity, the TLS was called “immature”. Of note, mature TLS displaying prominent germinal centers on HES staining were systematically confirmed with CD23 staining.

Immunohistochemistry stainings

All stainings were carried out on 3 micrometers paraffin slides using a Ventana Discovery Ultra platform (Ventana, Roche Diagnostics). Double immunohistochemistry was performed on all cases with i) CD3 (2GV6, Ventana) combined to CD20 (L26, Ventana) and ii) CD8 (C8/144B, Dako) combined to PD-L1 (QR1, Diagnostics). Stainings were performed with the protocol RUO discovery universal according to the manufacturer’s recommendations with the detection kits OmniMap anti-Rb HRP (760-4311, Ventana) and OmniMap anti-Ms HRP (760-4310, Ventana). The slides were scanned using the PerkinElmer Vectra Polaris System. The double CD20-CD23 immunohistochemistry staining was performed with the primary antibodies CD20 (clone L26, Ventana) and CD23 (clone 1B12, Novocastra). The procedure was performed with a Ventana Benchmark Ultra system (Ventana, Roche Diagnostics) using the Ultraview AP RED and Optiview DAB detection kits (Ventana) following the manufacturer’s recommendations (double stain oDAB-uRED v5 protocol, Ventana).

Assessment of the inter-rater agreement of the pathological assessment

The reproducibility to assess the TLS status of tumor samples with the pathology method was tested by training a third senior pathologist (IS) for TLS screening on a set of 15 samples. The trained pathologist subsequently analyzed blindly 150 tumor samples, selected randomly among tumor samples including 102 biopsies and 48 surgical specimens. The Cohen's kappa coefficient (κ) test was used to measure inter-rater reliability for the following criteria: 1) presence of TLS and 2) maturity of TLS (Supplementary Table 4). The inter-rater agreement rate was 0.7988 (Cohen's Kappa score, CI95: 0.7082-0.8892) for the presence of TLS and 0.7317 to evaluate the maturity of the TLS (range 0.5111-1.0) (Supplementary Table 4).

Multiplex immunohistofluorescence assay (Figure 1)

Multiplexed immunohistofluorescence was performed on TLS-positive cases (identified with HES and CD3/CD20 stainings) using the following antibodies CD20 (L26, Ventana), CD23 (SP23, Ventana), CD21 (2G9, Ventana), CD4 (4B12, Novocastra), CD8 (C8/144B, Dako). Bound primary antibodies were detected using OmniMap anti-Rb HRP (760-4311, Ventana) and OmniMap anti-Ms HRP (760-4310, Ventana) detection kits followed by TSA opal fluorophores (Opal 480, Opal 520, Opal 570, Opal 620 and Opal 690, Akoya Bioscience). The slides were counterstained with spectral DAPI (Akoya Bioscience) and cover-slipped. The slides were scanned using the PerkinElmer Vectra Polaris System, and the multispectral images obtained were unmixed using spectral libraries that were previously built from images stained for each fluorophore (monoplex), using the inForm Advanced Image Analysis software (inForm 2.4.1, Akoya Bioscience) combined with Opal detection kit (Akoya Bioscience).

Concordance of IHC versus IF screenings

All samples were analysed by IF in this study as previously described¹¹. A systematic comparison of results achieved with the double CD20/CD23 immunohistochemistry versus IF was performed with a set of 63 TLS-positive samples. The Kappa concordance score was 0.7914 (CI95: 0.6343-0.9484) (Supplementary Table 5).

PD-L1 scoring

For all tumors, the PD-L1 status was determined with both the TPS (tumor positive score) and CPS (combined positive score) following the guidelines. For the TPS, only viable tumor cells displaying partial or complete staining for PD-L1 membrane expression were considered relative to the total number of tumor cells. Positive immune cells and neoplastic cells showing only cytoplasmic staining were excluded²³. For the CPS, all PD-L1-positive cells were considered, including viable tumor cells, lymphocytes, and macrophages, relative to the total number of tumor cells. Only complete or partial membranous staining was considered, but not cytoplasmic staining²⁴.

Semi-automated and quantitative analysis of tumor surface and T-cell infiltrate

Stained slides were digitized with a multispectral slide-imaging platform (Vectra Polaris, Akoya Bioscience). Tumor surfaces were assessed with ImageJ software after manual

annotation of the scanned slide by a pathologist (LV, FLL) to calculate the TLS density (defined as the number of TLS per mm² of tumor surface). The density of CD8+ T cells per sample was semi-automatically assessed using Inform software (Akoya Bioscience, version 2.4.1) after tissue segmentation and digital cell phenotyping.

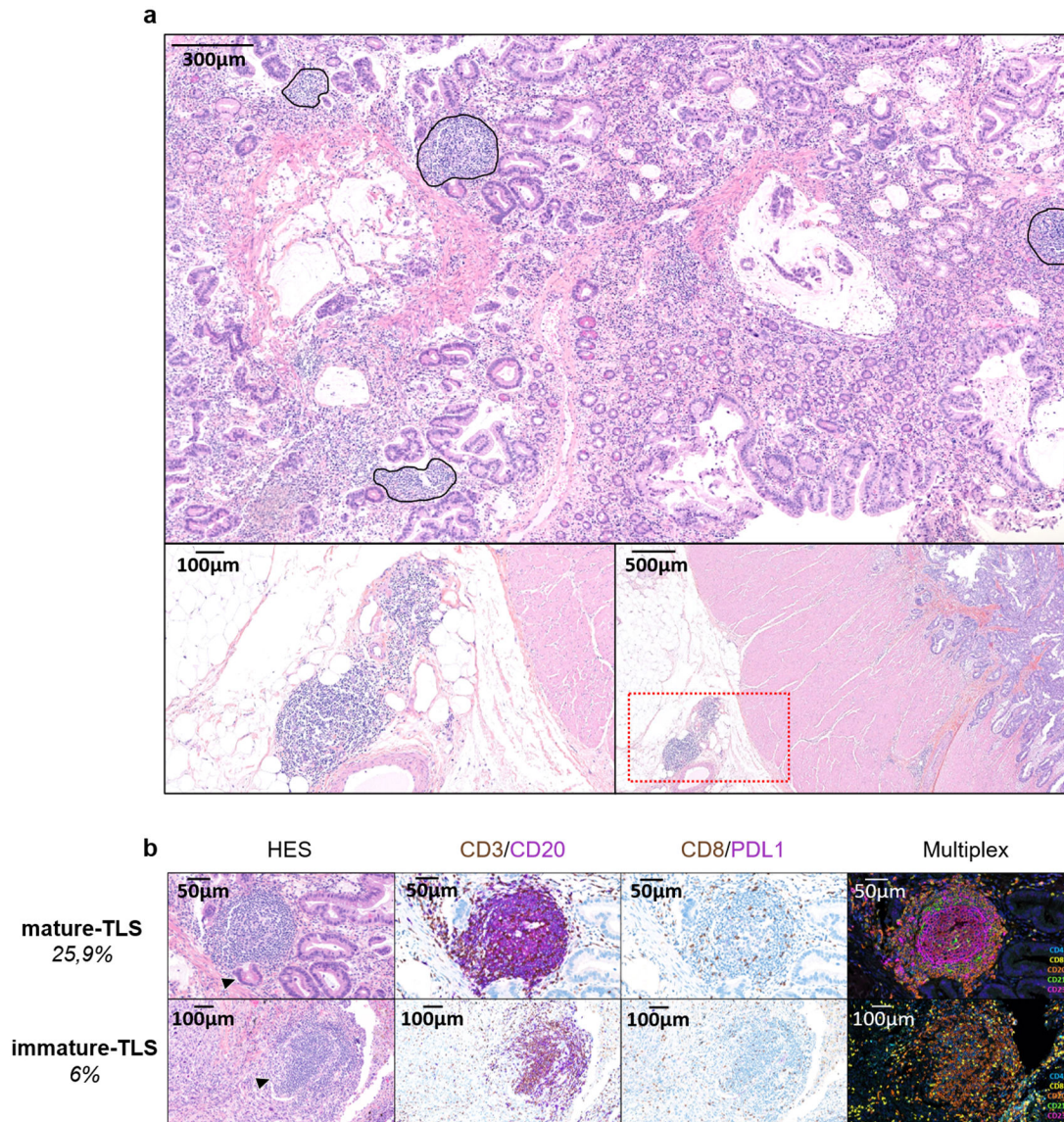
Tumor mutational burden (TMB)

The TMB was assessed using exome sequencing as previously described²⁵. To assess a clinically applicable cutoff point, we assessed TMB as a dichotomous variable, with TMB-high defined as at least 10 mutations per megabase.

Statistics and reproducibility

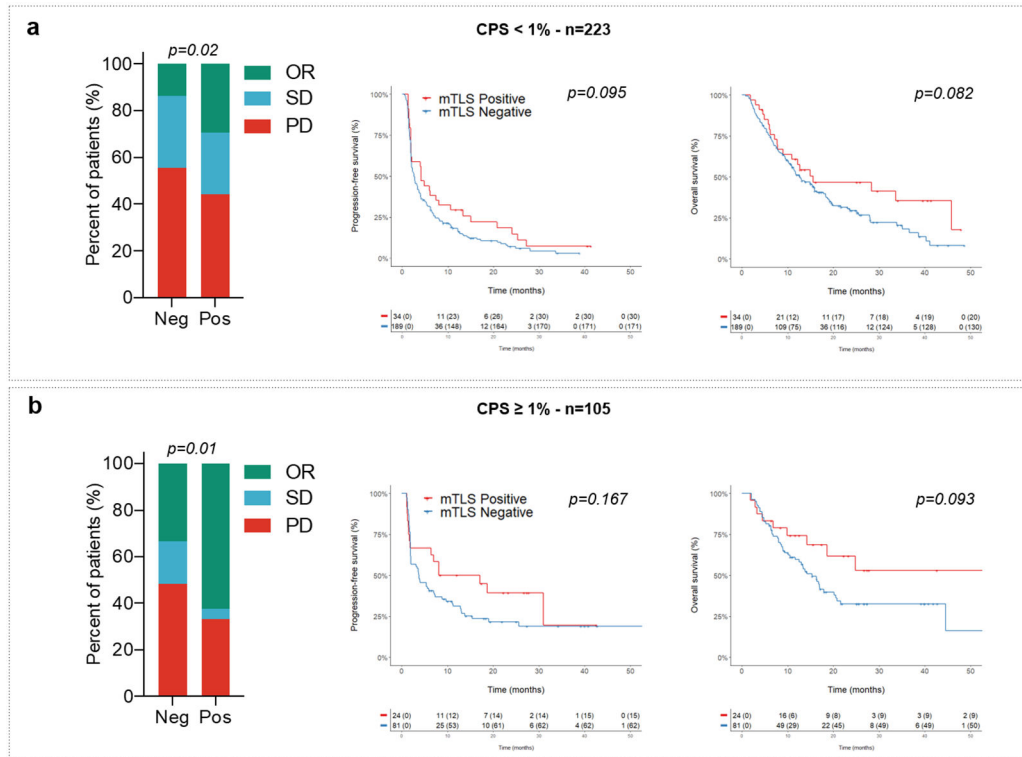
Patients who were treated with immune checkpoint inhibitors and had available tissue material from 2 biomarker prospective studies were included for analyses (NCT02534649: discovery cohort, NCT02517892: validation cohort B). Sample sizes for each of the 2 studies are justified in the sample size justification section of the respective protocols. For validation cohort A, patients from Clinique Marzet (Pau, France) who were treated with immune checkpoint inhibitors and had available tissue material were included for analyses provided they received first infusion before 31 December 2018 in order to ensure sufficient follow-up. Patients who did not have at least one imaging tumor evaluation performed after immunotherapy onset were excluded from the data set. The reproducibility to assess the TLS status of tumor samples was evaluated by assessing the inter-rater agreement within three independent pathologists as described above (Assessment of the inter-rater agreement of the pathological assessment). The data presented in the main Figures using multiplexed immunofluorescence analysis represents multiple tumor specimens from each tumor cohort analyzed in one experimental run. This is typical for human tumor tissue studies where the same tissue area/ exact cells cannot be analyzed more than once and replicates may introduce variations due to tissue heterogeneity or spatial variation. The cutoff date for statistical analysis of baseline demographic data and clinical outcome was 03/31/2020. Survival rates were estimated using the Kaplan–Meier method. Descriptive statistics were used to describe the distribution of variables in the population. Differences between groups were evaluated by the chi-squared test or Fisher’s exact test for categorical variables and by Student’s t-test for continuous variables. Prognostic factors were identified by univariate and multivariate analyses using a Cox regression model. Variables tested in the univariate analysis included age, gender, tumor type, number of previous lines of treatment, performance status, PD-L1 expression status as assessed by the tumor proportion score (TPS), CD8+ T-cell density, and mature TLS density. Variables associated with PFS and OS with a p-value <0.05 in the univariate analysis were included in the multivariate analysis. The univariate and multivariate analyses were performed using SPSS 25.0 statistical software (IPSS Inc., Chicago, USA). All statistical tests were two-sided, and p<0.05 indicated statistical significance. The inter-rater agreement score was assessed by Cohen’s kappa score.

Extended Data

**Extended Data Fig. 1. Assessment of the presence of TLS and their maturation stage in tumors.**

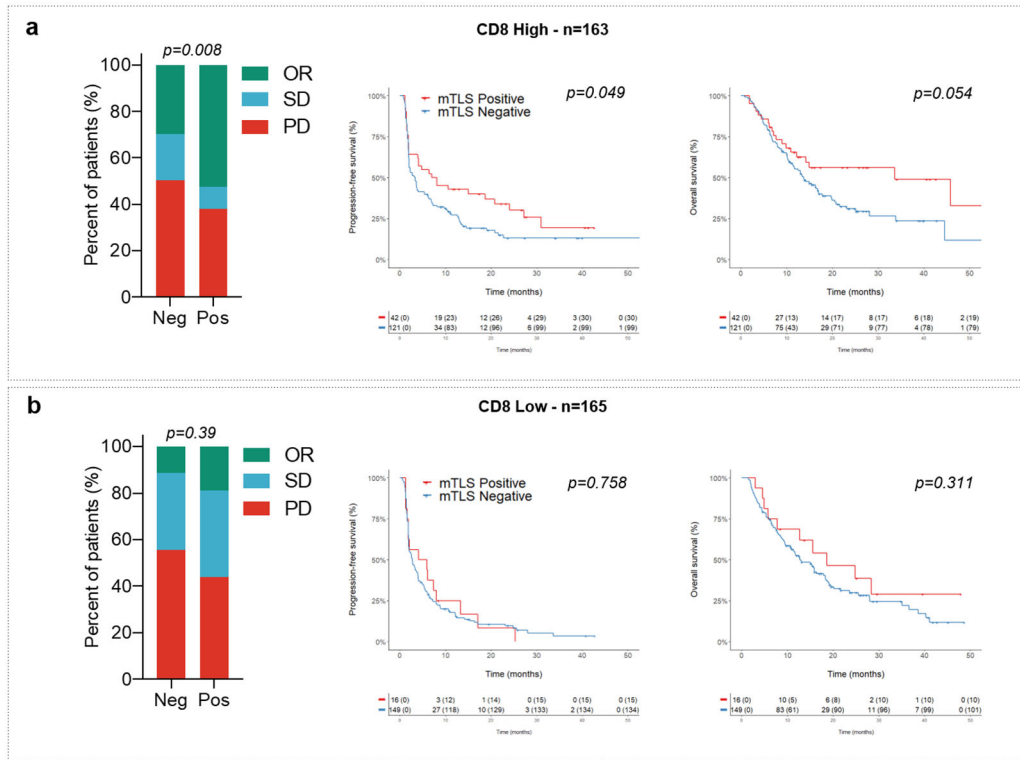
a: This is a TLS-positive primary pancreatic adenocarcinoma associated with a T CD8+ lymphocyte density of $154/\text{mm}^2$ and negative for PD-L1. The TLS are delineated with the black lines on the HES slide, highlighting their vicinity to tumor cells. Scale bar indicates $300\mu\text{m}$ in size. Representative of 540 tumors analyzed (Discovery cohort $n=328$, validation cohort A $n=131$, validation cohort B $n=81$). **b:** This panel shows representative examples of immature and mature TLS observed in tumor samples. Upper panel: This mature TLS is detected in a primary pancreatic adenocarcinoma associated with a T CD8+ lymphocyte density of $154/\text{mm}^2$ and negative for PD-L1. Mature TLS are defined by the presence of a network of CD23-positive dendritic cells on immunofluorescence (note that in this case, the presence of a germinal center visible on the HES was already diagnostic of a mature TLS). Lower panel: The picture shows an immature TLS detected in a primary adenocarcinoma

of the lung concomitantly showing a high T CD8+ lymphocyte infiltrate of 372/mm² and a PD-L1 TPS score of 1%. The tumor was only associated with immature TLS displaying no germinal center and no network of CD23-positive dendritic cells on immunofluorescence. Representative of 540 tumors analyzed (Discovery cohort n=328, validation cohort A n=131, validation cohort B n=81). The pictures from the left to right column correspond to 1) Hematoxylin Eosin Saffron (HES) staining, 2) Double immunohistochemistry staining of CD3/CD20 (CD3 in brown, CD20 in purple), 3) Double immunohistochemistry staining of CD8/PD-L1 (CD8 in brown, PD-L1 in purple), 4) Multiplex immunofluorescence assay of CD4 (blue), CD8 (yellow), CD20 (orange), CD21 (green) and CD23 (pink). The scale bars on the HES images indicate 50µm and 100µm for the upper and lower panels, respectively. Black crossed arrows highlight the tumor cells in the samples.

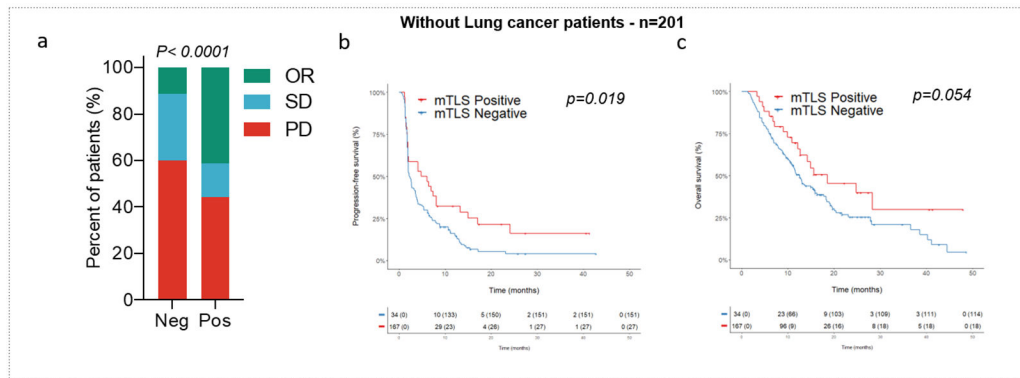


Extended Data Fig. 2. Predictive value of TLS status according to CPS PD-L1 scores.

Objective response rates (OR: objective response, SD: stable disease; PD: progressive disease; chi squared (χ^2) test) and Kaplan-Meier curves of progression-free survival (log-rank test) and overall survival (log-rank test) of 328 cancer patients treated with anti-PD1/PD-L1 antagonists according to CPS PD-L1 scores (a: CPS PD-L1 <1, N=223 patients; b: CPS PD-L1 \geq 1, N=105 patients) and TLS status (red curve: mature-TLS positive tumors; blue line: mature-TLS negative tumors).

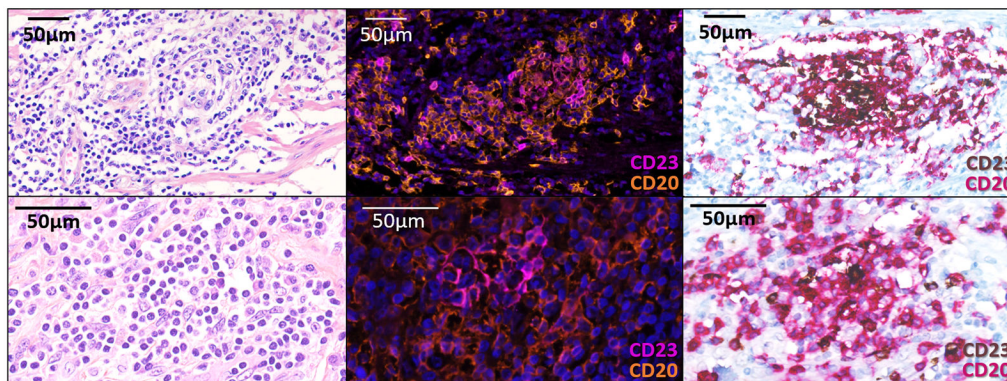


Extended Data Fig. 3. Predictive value of TLS status according to T CD8 cell density. Objective Response rates (OR: objective response, SD: stable disease, PD: progressive disease; chi squared (χ^2) test) and Kaplan-Meier curves of progression-free (log-rank test) and overall survival (log-rank test) of 328 cancer patients treated with anti-PD1/PD-L1 antagonists according to T CD8+ cell density (a: low density, N=165 patients; b: high density, N=163 patients) and TLS status (red curve: mature-TLS positive tumors; blue line: mature-TLS negative tumors).



Extended Data Fig. 4. Outcome of cancer patients (non-small cell lung cancer excluded) according to TLS status
 a) Objective Response rates (OR: objective response, SD: stable disease, PD: progressive disease; chi squared (χ^2) test) and Kaplan-Meier curves (log-rank test) of progression-free (b) and overall survival (c) of 201 cancer patients (all tumor types except non-small cell

lung cancer) treated with anti-PD1/PD-L1 antagonists according to TLS status (red curve: mature-TLS positive tumors; blue line: mature-TLS negative tumors).



Extended Data Fig. 5. Comparison of the TLS screening with pathology and immunohistochemistry pathology versus the screening with immunofluorescence (method by Petitprez et al).

First line: conspicuous mature TLS with CD23+ follicular dendritic cells network. Second line: mature TLS defined by isolated CD23+ cell displaying dendritic morphology. Pictures from the left to right column correspond to 1) Hematoxylin Eosin Saffron (HES) staining, 2) Multiplex immunofluorescence assay of CD23 (pink) and CD20 (orange), 3) Double immunohistochemistry staining of CD23/CD20 (CD23 in brown, CD20 in red). The scale bars on the HES images indicate 50µm in size. Representative of 540 tumors analyzed (Discovery cohort n=328, validation cohort A n=131, validation cohort B n=81).

Supplementary Material

Refer to Web version on PubMed Central for supplementary material.

ACKNOWLEDGMENTS

This study was funded by Astra Zeneca.

Data Availability

The datasets that support the findings of this study are not publicly available due to information that could compromise research participant consent. According to French/ European regulations, any re-use of the data must be approved by the ethic committee. Each request for access to the dataset (including the images) will be granted after request sent to the corresponding author (AI) and approval by the ethic committee and after information of the patients. Source Data are available for this study.

REFERENCES

1. Vaddepally RK, Kharel P, Pandey R, Garje R, Chandra AB. Review of Indications of FDA-Approved Immune Checkpoint Inhibitors per NCCN Guidelines with the Level of Evidence. *Cancers (Basel)*. 2020 Mar 20;12(3).

2. Davis AA, Patel VG. The role of PD-L1 expression as a predictive biomarker: an analysis of all US Food and Drug Administration (FDA) approvals of immune checkpoint inhibitors. *J Immunother Cancer*. 2019;7(1):278. [PubMed: 31655605]
3. Cassetta L, Kitamura T. Targeting Tumor-Associated Macrophages as a Potential Strategy to Enhance the Response to Immune Checkpoint Inhibitors. *Front Cell Dev Biol*. 2018;6:38. [PubMed: 29670880]
4. Schalper KA, Carleton M, Zhou M, et al. Elevated serum interleukin-8 is associated with enhanced intratumor neutrophils and reduced clinical benefit of immune-checkpoint inhibitors. *Nat Med*. 2020;26(5):688–692. [PubMed: 32405062]
5. Sautès-Fridman C, Petitprez F, Calderaro J, Fridman WH. Tertiary lymphoid structures in the era of cancer immunotherapy. *Nat Rev Cancer*. 2019;19(6):307–325. [PubMed: 31092904]
6. Ladányi A, Kiss J, Mohos A, Somlai B, Liskay G, Gilde K, Fejös Z, Gaudi I, Dobos J, Tímár J. Prognostic impact of B-cell density in cutaneous melanoma. *Cancer Immunol Immunother*. 2011 Dec;60(12):1729–38.4 [PubMed: 21779876]
7. Messina JL, Fenstermacher DA, Eschrich S, Qu X, Berglund AE, Lloyd MC, Schell MJ, Sondak VK, Weber JS, Mulé JJ. 12-Chemokine gene signature identifies lymph node-like structures in melanoma: potential for patient selection for immunotherapy? *Sci Rep*. 2012;2:765. [PubMed: 23097687]
8. Goc J, Germain C, Vo-Bourgais TK, Lupo A, Klein C, Knockaert S, de Chaisemartin L, Ouakrim H, Becht E, Alifano M, Validire P, Remark R, Hammond SA, Cremer I, Damotte D, Fridman WH, Sautès-Fridman C, Dieu-Nosjean MC. Dendritic cells in tumor-associated tertiary lymphoid structures signal a Th1 cytotoxic immune contexture and license the positive prognostic value of infiltrating CD8+ T cells. *Cancer Res*. 2014 Feb 1;74(3):705–15. [PubMed: 24366885]
9. Behr DS, Peitsch WK, Hametner C, et al. (2014) Prognostic value of immune cell infiltration, tertiary lymphoid structures and PD-L1 expression in Merkel cell carcinomas. *Int J Clin Exp Pathol* 7:7610–7621. [PubMed: 25550797]
10. Caro GD, Bergomas F, Grizzi F, et al. (2014) Occurrence of tertiary lymphoid tissue is associated with T-cell infiltration and predicts better prognosis in early-stage colorectal cancers. *Clin Cancer Res* 20:2147–2158. [PubMed: 24523438]
11. Petitprez F, de Reyniès A, Keung EZ, Chen TW, Sun CM, Calderaro J, Jeng YM, Hsiao LP, Lacroix L, Bougouïn A, Moreira M, Lacroix G, Natario I, Adam J, Lucchesi C, Laizet YH, Toulmonde M, Burgess MA, Bolejack V, Reinke D, Wani KM, Wang WL, Lazar AJ, Roland CL, Wargo JA, Italiano A, Sautès-Fridman C, Tawbi HA, Fridman WH. B cells are associated with survival and immunotherapy response in sarcoma. *Nature*.2020;577(7791):556–560 [PubMed: 31942077]
12. Cabrita R, Lauss M, Sanna A, Donia M, Skaarup Larsen M, Mitra S, Johansson I, Phung B, Harbst K, Vallon-Christersson J, van Schoiack A, Lövgren K, Warren S, Jirstrom K, Olsson H, Pietras K, Ingvar C, Isaksson K, Schadendorf D, Schmidt H, Bastholt L, Carneiro A, Wargo JA, Svane IM, Jönsson G. Tertiary lymphoid structures improve immunotherapy and survival in melanoma. *Nature*. 2020;577(7791):561–565. [PubMed: 31942071]
13. Helmink BA, Reddy SM, Gao J, Zhang S, Basar R, Thakur R, Yizhak K, Sade-Feldman M, Blando J, Han G, Gopalakrishnan V, Xi Y, Zhao H, Amaria RN, Tawbi HA, Cogdill AP, Liu W, LeBleu VS, Kugeratski FG, Patel S, Davies MA, Hwu P, Lee JE, Gershenwald JE, Lucci A, Arora R, Woodman S, Keung EZ, Gaudreau PO, Reuben A, Spencer CN, Burton EM, Haydu LE, Lazar AJ, Zapassodi R, Hudgens CW, Ledesma DA, Ong S, Bailey M, Warren S, Rao D, Krijgsman O, Rozeman EA, Peeper D, Blank CU, Schumacher TN, Butterfield LH, Zelazowska MA, McBride KM, Kalluri R, Allison J, Petitprez F, Fridman WH, Sautès-Fridman C, Hacohen N, Rezvani K, Sharma P, Tetzlaff MT, Wang L, Wargo JA. B cells and tertiary lymphoid structures promote immunotherapy response. *Nature*. 2020;577(7791):549–555 [PubMed: 31942075]
14. Tsou P, Katayama H, Ostrin EJ, Hanash SM The Emerging Role of B Cells in Tumor Immunity. *Cancer Res*. 2016;76:5597–5601. [PubMed: 27634765]
15. Bruno TC. New predictors for immunotherapy responses sharpen our view of the tumour microenvironment. *Nature*. 2020;577(7791):474–476. [PubMed: 31965091]

16. Kroeger DR, Milne K, Nelson BH. Tumor-Infiltrating Plasma Cells Are Associated with Tertiary Lymphoid Structures, Cytolytic T-Cell Responses, and Superior Prognosis in Ovarian Cancer. *Clin Cancer Res.* 2016;22:3005–15. [PubMed: 26763251]
17. Germain C, Gnjatic S, Tamzalit F, Knockaert S, Remark R, Goc J, Lepelley A, Becht E, Katsahian S, Bizouard G, Validire P, Damotte D, Alifano M, Magdeleinat P, Cremer I, Teillaud JL, Fridman WH, Sautès-Fridman C, Dieu-Nosjean MC. Presence of B cells in tertiary lymphoid structures is associated with a protective immunity in patients with lung cancer. *Am J Respir Crit Care Med.* 2014 Apr 1;189(7):832–44. [PubMed: 24484236]
18. Montfort A, Pearce O, Maniati E, Vincent BG, Bixby L, Böhm S, Dowe T, Wilkes EH, Chakravarty P, Thompson R, Topping J, Cutillas PR, Lockley M, Serody JS, Capasso M, Balkwill FR. A Strong B-cell Response Is Part of the Immune Landscape in Human High-Grade Serous Ovarian Metastases. *Clin Cancer Res.* 2017 Jan 1;23(1):250–262. [PubMed: 27354470]
19. Kalergis AM, Ravetch JV. Inducing tumor immunity through the selective engagement of activating Fcγ receptors on dendritic cells. *J Exp Med.* 2002 Jun 17;195(12):1653–9. [PubMed: 12070293]
20. Fridman WH et al., *J Exp Med*, 2020, in press
21. Lu Y, Zhao Q, Liao JY, Song E, Xia Q, Pan J, Li Y, Li J, Zhou B, Ye Y, Di C, Yu S, Zeng Y, Su S. Complement Signals Determine Opposite Effects of B Cells in Chemotherapy-Induced Immunity. *Cell.* 2020;180(6):1081–1097 [PubMed: 32142650]
22. Schwartz LH, Litière S, de Vries E, Ford R, Gwyther S, Mandrekar S, Shankar L, Bogaerts J, Chen A, Dancy J, Hayes W, Hodi FS, Hoekstra OS, Huang EP, Lin N, Liu Y, Therasse P, Wolchok JD, Seymour L. RECIST 1.1-Update and clarification: From the RECIST committee. *Eur J Cancer.* 2016;62:132–7. [PubMed: 27189322]
23. Vigliar E, Malapelle U, Iaccarino A, Acanfora G, Pisapia P, Clery E, De Luca C, Bellevicine C, Troncone G. PD-L1 expression on routine samples of non-small cell lung cancer: results and critical issues from a 1-year experience of a centralised laboratory. *J Clin Pathol.* 2019; 72:412–417 [PubMed: 30846480]
24. Balar AV, Castellano D, O'Donnell PH, Grivas P, Vuky J, Powles T, Plimack ER, Hahn NM, de Wit R, Pang L, Savage MJ, Perini RF, Keefe SM, Bajorin D, Bellmunt J. First-line pembrolizumab in cisplatin-ineligible patients with locally advanced and unresectable or metastatic urothelial cancer (KEYNOTE-052): a multicentre, single-arm, phase 2 study. *Lancet Oncol.* 2017;18:1483–1492 [PubMed: 28967485]
25. Koepfel F, Bobard A, Lefebvre C, Pedrero M, Deloger M, Boursin Y, Richon C, Chen-Min-Tao R, Robert G, Meurice G, Rouleau E, Michiels S, Massard C, Scoazec JY, Solary E, Soria JC, André F, Lacroix L. Added Value of Whole-Exome and Transcriptome Sequencing for Clinical Molecular Screenings of Advanced Cancer Patients With Solid Tumors. *Cancer J.* 2018 Jul/Aug;24(4):153–162. [PubMed: 30119077]

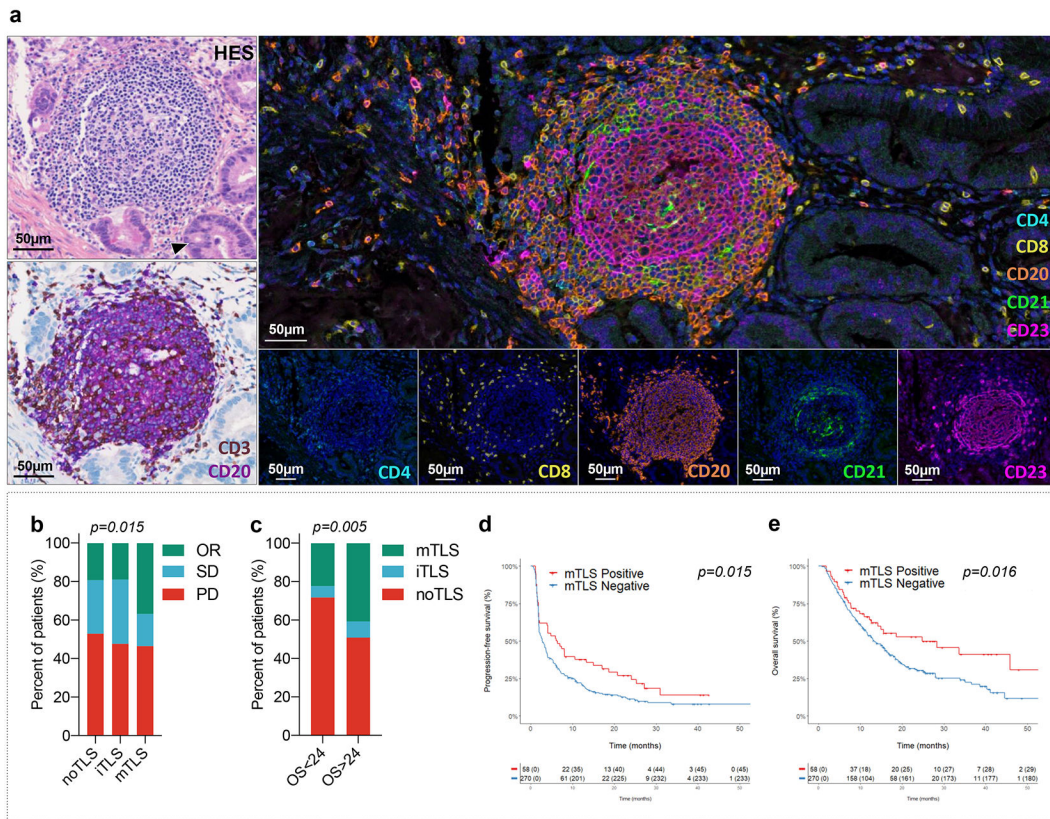


Figure 1. Mature TLS are predictive of outcome in cancer patients treated with immune-checkpoint inhibitors.

a, The presence of TLS in tumors was systematically screened with a Hematoxylin Eosin Saffron (HES) staining and double immunohistochemistry staining of CD3-CD20 (CD3 and CD20 stained in brown and purple, respectively). PD-L1 status was assessed with a double immunohistochemistry staining of CD8/PD-L1 (CD8 and PD-L1 stained in brown and purple, respectively). The maturity of TLS was assessed in TLS positive tumors with a multiplex immunofluorescence assay combining CD4, CD8, CD20, CD21 and CD23 markers. This illustrated case is a primary pancreatic adenocarcinoma associated with mature TLS displaying a prominent germinal center on HES staining. Representative of 540 tumors analyzed (Discovery cohort n=328, validation cohort A n=131, validation cohort B n=81). This tumor was negative for PD-L1 and displayed a T-cell CD8+ lymphocytes density of 154/mm². Immunofluorescence assay show a dense network of CD23+ follicular dendritic cells within the germinal center. The scale bar indicates 50µm in size. Black cropped arrow highlights the tumor cells in the sample. Images at the bottom show the expression of each single marker assessed with its corresponding fluorescence spectrum.

b, Response rate as defined per RECIST criteria according to the TLS status: absence (no TLS, N=223 patients), immature TLS (iTLS, N=21 patients) or mature TLS (mTLS, N=84 patients). PD is indicative of progressive disease, SD of stable disease and OR of objective response as per RECIST 1.1 criteria. [chi squared (χ^2) test]

c, Proportion of patients characterized by the absence or presence of either iTLS or mTLS according to overall survival endpoint (OS < 24 months versus > 24 months from immunotherapy onset, chi-squared test) [panels (B,C), N = 328 patients]

d, Kaplan-Meier curves of progression-

free survival and overall survival in the discovery cohort of 328 cancer patients treated with anti-PD1/PD-L1 antagonists according to the mature TLS status (red curve: mature-TLS enriched tumors; blue curve: mature-TLS negative tumors). [log-rank test]

Author Manuscript

Author Manuscript

Author Manuscript

Author Manuscript

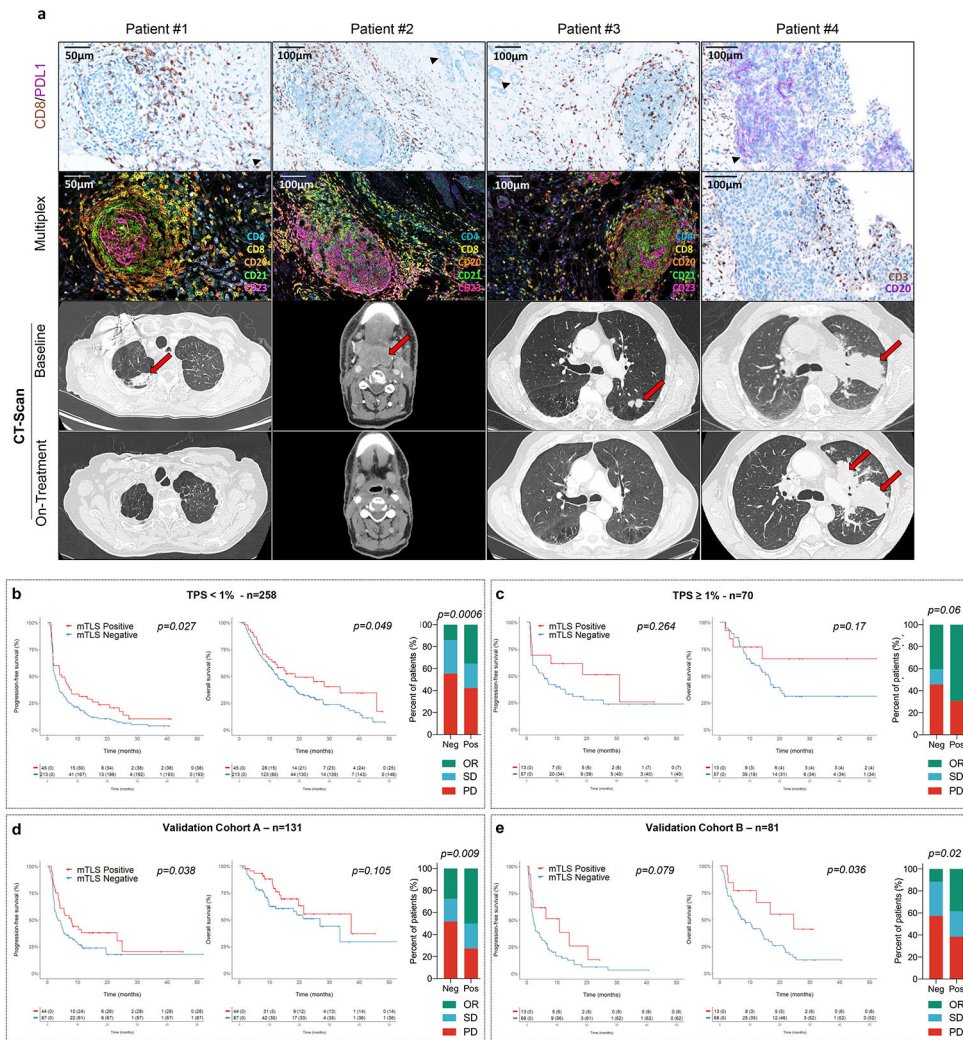


Figure 2. Mature TLS are predictive of response to immune-checkpoint inhibition independently of the PD-L1 expression status.

a. Panel A: For each case, from top to bottom, 1) Double staining of CD8/PD-L1 (CD8 in brown, PD-L1 in purple); 2) Multiplex immunofluorescence assay of CD4 (blue), CD8 (yellow), CD20 (orange), and CD23 (pink); 3) and 4) Computed Tomography scan obtained at baseline and 8-16 weeks after treatment onset. **Patient #1:** Near complete response in a case of mature TLS+ metastasis of a lung adenocarcinoma with a CD8+ T lymphocytes density of 159/mm² and a negative PD-L1 status. **Patient #2:** Complete response in a case of mature TLS+ metastasis of a pharyngeal squamous cell carcinoma negative for PD-L1 associated with a T-CD8 lymphocytes density of 124/mm². **Patient #3:** Near complete response in a case of mature TLS+ microsatellite stable (MSS) colorectal adenocarcinoma associated with a T-CD8+ lymphocytes density of 115/mm² and with a low PD-L1 rate (TPS score = 1%). **Patient #4:** Progressive disease in a patient with advanced lung adenocarcinoma showing high expression of PD-L1 and no detectable TLS (Representative of tumor samples and imaging of N = 4 patients from 540 tumors analyzed [Discovery cohort n=328, validation cohort A n=131, validation cohort B n=81]). **b.** On the left part, the histogram highlights the response rates achieved in patients with PDL1-negative tumors

(defined as a TPS score < 1%, N=258 patients) according to the absence (no mTLS) or presence of mTLS. On the right part, from the left to right the Kaplan-Meier curves depict the progression-free survival and overall survival of the patients with PDL1-negative tumors according to their mTLS status. [log-rank test] **c**, On the left part, the histogram highlights the different response rates in patients with PDL1-positive tumors (defined as a TPS score > 1%, N=70 patients) according to the absence or presence of mTLS. On the right part, from the left to right the Kaplan-Meier curves depict the progression-free survival and overall survival of the patients with PD-L1-positive tumors according to their mTLS status d-e) In validation cohort A (N=131 patients) and in validation cohort B consisting (N=81 patients) , all treated with PD(L)1 antagonists, (left) illustration of response rate as defined per RECIST criteria according to the absence or presence of mature TLS (mTLS) and (right) Kaplan-Meier curves of progression-free survival and overall survival of cancer patients according to the absence or presence of mTLS. [log-rank test]

Abbreviations: SD: stable disease, OR: objective response, PD: progressive disease, mTLS: mature TLS.

Table 1.

Discovery cohort: clinical characteristics of patients with TLS-positive tumors (according to TLS status)

	Presence of TLS (n=105)	No TLS (n=223)
Median Age	62 (range 35-84)	62 (range 20-88)
Gender		
Male	57 (53%)	139 (62%)
Female	48 (47%)	84 (38%)
Tumor Type		
Non-small cell lung cancer	37 (37.1%)	90 (41.2%)
Soft-tissue sarcomas	8 (7.6%)	38 (17%)
Bladder cancer	15 (14.3%)	16 (7.2%)
Colorectal cancer	11 (10.5%)	16 (7%)
Head and neck carcinomas	5 (4.8%)	7 (3.1%)
Renal carcinoma	2 (1.9%)	8 (3.6%)
Breast carcinoma	1 (1%)	6 (2.7%)
Other	26 (22.8%)	42 (17.9%)
Performance status		
1	97 (92.4%)	207 (92.8%)
> 1	8 (7.6%)	16 (7.2%)
Previous lines of treatment		
1	65 (61.9%)	138 (61.9%)
> 1	40 (38.1%)	85 (38.1%)
Treatment		
Anti-PD1	56 (53.3%)	139 (62.3%)
Anti-PD-L1	38 (36.2%)	62 (27.8%)
Combination PD1 or anti-PD-L1 + another immune checkpoint inhibitor	11 (10.5%)	22 (9.9%)

* **Other tumors:** thyroid carcinoma, gastrointestinal stromal tumor, cholangiocarcinoma, pancreatic adenocarcinoma, anal carcinoma, cervical cancer, ovarian cancer, vulvar carcinoma, endometrial carcinoma, cervical cancer, gastric carcinoma.

Table 2.

Response rate according to the density of mature TLS in patients depending on PD-L1 status and CD8 density*

		mature-TLS density				
TPS PD-L1 Score			Low	High	Total	p value
<1%	RECIST	PD	118 (55.4%)	19 (42.2%)	137	0.0006
		SD	65 (30.5%)	10 (22.2%)	75	
		CR+PR	30 (14.1%)	16 (35.6%)	46	
Total			213	45	258	
1%	RECIST	PD	26 (45.6%)	4 (30.8%)	30	0.06
		SD	8 (14%)	0	8	
		CR+PR	23 (40.4%)	9 (69.2%)	32	
Total			57	13	70	
Total	RECIST	PD	144 (53.3%)	23 (39.7%)	167	0.0001
		SD	73 (27%)	10 (17.2%)	83	
		CR+PR	53 (19.6%)	25 (43.1%)	78	
Total			270	58	328	
CPS PD-L1 Score						
<1%	RECIST	PD	105 (55.6%)	15 (44.1%)	120	0.02
		SD	58 (30.7%)	9 (26.5%)	67	
		CR+PR	26 (13.8%)	10 (29.4%)	36	
Total			189	34	223	
1%	RECIST	PD	39 (48.1%)	8 (33.3%)	47	0.001
		SD	15 (18.5%)	1 (4.2%)	16	
		CR+PR	27 (33.4%)	15 (62.5%)	42	
Total			81	24	105	
Total	RECIST	PD	144 (53.3%)	23 (39.7%)	167	0.0001
		SD	73 (27%)	10 (17.2%)	83	
		CR+PR	53 (19.6%)	25 (43.1%)	78	
Total			270	58	328	
CD8 density						
Low			Low	High		p value
Low	RECIST	PD	83 (55.7%)	7 (43.8%)	90	0.39
		SD	49 (32.9%)	6 (37.5%)	55	
		CR+PR	17 (11.4%)	3 (18.8%)	20	
Total			149	16	165	
High	RECIST	PD	61 (50.4%)	16 (38.1%)	77	0.008
		SD	24 (19.8%)	4 (9.5%)	28	
		CR+PR	36 (29.8%)	22 (52.4%)	58	
Total			121	42	163	

TPS PD-L1 Score		mature-TLS density			p value
		Low	High	Total	
Total	RECIST	PD	144 (53.3%)	23 (39.37)	0.0001
		SD	73 (27%)	10 (17.2%)	
		CR+PR	53 (19.6%)	25 (43.1%)	
Total			270	58	328

* Statistical test: Pearson's chi-squared test

Author Manuscript

Author Manuscript

Author Manuscript

Author Manuscript

Table 3.

Univariate and multivariate Cox analyses for progression-free and overall survival

Univariate analysis for PFS (n=328)				Multivariate analysis for PFS (n=328)			
Variable		Median (Months)	95% CI	p value	HR	95% CI	p value
Whole population		3.3	[2.5-4.1]	-	-		
Performance status (ECOG)	1	3.6	[2.9-4.3]	<0.0001	0.4	[0.3-0.6]	<0.0001
	> 1	1.6	[1.1-2.1]		1		
Cancer Type	NSCLC	4	[2.3-5.7]	0.003	-		
	Other	2.6	[1.9-3.3]				
Previous lines of treatment	1	3.9	[2.9-4.8]	0.003	-		
	> 1	2.5	[1.9-3.1]				
TPS score (%)	< 1	2.7	[1.9-3.5]	<0.0001	1.7	[1.3-2.5]	0.001
	1	7.0	[1.4-12.6]		1		
CD8 density	Low density	2.7	[1.7-3.6]	0.005	-		
	High density	3.7	[1.9-5.4]				
Presence of mature TLS	No	2.7	[1.9-3.5]	0.015	1.4	[1.1-2.0]	0.04
	Yes	6.1	[1.9-10.2]		1		
Univariate analysis for OS (n=328)				Multivariate analysis for OS (n=328)			
Variable		Median (Months)	95% CI	p value	HR	95% CI	p value
Whole population		14.9	[12.9-16.9]	-	-		
Performance status	1	15.6	[12.9-18.3]	<0.0001	0.32	[0.20-0.51]	<0.0001
	> 1	5	[2.1-7.9]		1		
Cancer Type	NSCLC	16.8	[13-20.6]	0.06	-		
	Other	12.9	[10.7-15.1]				
TPS score (%)	< 1	13.1	[10.8-15.4]	0.07	-		
	1	16.9	[12.8-20.9]				
CD8 density	Low	13.1	[10.2-15.9]	0.18	-		
	High	14.9	[11.9-17.9]				
Presence of mature TLS	No	13.3	[11.1-15.5]	0.016	1.5	[1.1-2.3]	0.03
	Yes	24.8	[6.8-42.8]		1		

* Statistical test: Cox regression model